Available online at www.sciencedirect.com
ScienceDirect
Journal of Magnetic Resonance 186 (2007) 341–346
JMR Journal of Magnetic Resonance
www.elsevier.com/locate/jmr

Communication

4 T Actively detuneable double-tuned $^{1}H/^{31}P$ head volume coil and four-channel ^{31}P phased array for human brain spectroscopy

N.I. Avdievich *, H.P. Hetherington

Department of Radiology, Albert Einstein College of Medicine, Bronx, NY, USA
Gruss Magnetic Resonance Research Center, Bronx, NY, USA
Department of Neurosurgery, Yale University, MRRC/TAC, 300 Cedar Street, New Haven, CT 06520, USA

Received 2 August 2006; revised 9 February 2007
Available online 3 March 2007

Abstract

Typically ^{31}P *in vivo* magnetic resonance spectroscopic studies are limited by SNR considerations. Although phased arrays can improve the SNR; to date ^{31}P phased arrays for high-field systems have not been combined with ^{31}P volume transmit coils. Additionally, to provide anatomical reference for the ^{31}P studies, without removal of the coil or patient from the magnet, double-tuning ($^{31}P/^{1}H$) of the volume coil is required. In this work we describe a series of methods for active detuning and decoupling enabling use of phased arrays with double-tuned volume coils. To demonstrate these principles we have built and characterized an actively detuneable $^{31}P/^{1}H$ TEM volume transmit/four-channel ^{31}P phased array for 4 T magnetic resonance spectroscopic imaging (MRSI) of the human brain. The coil can be used either in volume-transmit/array-receive mode or in TEM transmit/receive mode with the array detuned. Threefold SNR improvement was obtained at the periphery of the brain using the phased array as compared to the volume coil.

Keywords: TEM coil; High field MRI/MRS; ^{31}P phased array; Actively detuneable $^{31}P/^{1}H$ volume coil

1. Introduction

Optimal signal-to-noise ratio (SNR) for *in vivo* studies is typically obtained when a homogeneous volume coil is used for transmission and a receive-only phased array is utilized for reception [1]. Although ^{31}P *in vivo* magnetic resonance spectroscopic imaging (MRSI) is often limited by the available SNR, there are few reports of the use of ^{31}P phased arrays to increase sensitivity for human brain studies [2,3]. Although receive-only ^{31}P phased arrays in combination with larger transmit-only surface coils have been reported [2,3]; to our knowledge their use with homogeneous transmit volume coils has not been yet reported. To provide high-resolution anatomical imaging and shimming with a homogeneous volume coil without removal of the coil or patient from the magnet, double-tuning of the transmit volume coil is required. To avoid interaction between volume and surface coils resonating at the same frequency, active detuning of both coils must be incorporated. In spite of the fact that ^{1}H and ^{31}P frequencies differ substantially at 4 T (170 MHz versus 69 MHz), interactions between the ^{1}H volume coil and the ^{31}P surface coils produces RF field distortions and, therefore, the volume coil is also required to be actively detuned at both frequencies. The presence of multiple surface coils and as a result, multiple cables connected to these coils, results in noise injection and cable interaction. This interaction, in turn, produces additional coil coupling and reduces the SNR. This problem is commonly dealt with by cable routing [1,4] and the use of lumped-element or coaxial tri-axial baluns [5]. Double-tuning of the volume coil further complicates this issue by inducing additional coupling between the elements of the ^{1}H volume coil and the ^{31}P phased array.

* Corresponding author. Address: Department of Neurosurgery, Yale University, MRRC/TAC, 300 Cedar Street, New Haven, CT 06520, USA. Fax: +1 203 785 6643.
E-mail address: nikolai.avdievich@yale.edu (N.I. Avdievich).

1090-7807/$ - see front matter © 2007 Elsevier Inc. All rights reserved.
doi:10.1016/j.jmr.2007.03.001

In this work we describe the design and construction of an actively detuneable $^{1}H/^{31}P$ double-tuned transverse electromagnetic (TEM) [6] transmit-receive volume coil and a ^{31}P receive-only phased array for ^{31}P spectroscopic imaging (SI) of the human brain at 4 T. Depending upon the target application (minimizing acquisition time (SENSE), maximizing SNR for peripheral or central locations) and hardware configuration (number of receiver channels), arrays with larger numbers of coils, differing geometries and sizes will most likely provide superior performance. An extensive discussion of the various design criteria for each specific application is not possible in this work, but has been discussed extensively elsewhere [1,7–18]. However, independent of the specific design of the array, isolation between the volume coil and the array is critical to maintaining SNR and B_1 field profiles. The new design of double-tuned tri-axial baluns, capable of producing high impedance between the two braids at both frequencies, allows us to effectively suppress shield currents and cable interactions at both 170 and 69 MHz.

2. Methods

2.1. Design of the RF coils and evaluation procedures

A double-tuned $^{31}P/^{1}H$ (69 MHz/170 MHz) TEM head coil was built using 24 coaxial resonant elements with alternate elements tuned to the two frequencies (^{31}P and ^{1}H) [6]. The coil measured 23.9 cm in length with an RF shield o.d. of 38 cm and an element i.d. (diameter at the centers of the elements) of 31.8 cm. To improve the RF homogeneity in the axial direction, the coil had a shielded back wall [6]. The volume coil was driven in quadrature using two-port drives for both frequencies (Fig. 1A). The ratios of unloaded to loaded Q-factors (Q_U/Q_L) measured on a human head for ^{1}H and ^{31}P portions of the TEM coil were 740/130 and 550/140, respectively. Active detuning of the volume coil at both frequencies was provided using PIN diodes similar to that described previously [19,20]. In these schemes, each resonant element of the TEM coil can be viewed as a separate resonant circuit consisting of an inductor and two variable coaxial capacitors connected in series. In previous work [19,20] the TEM volume coil was detuned by shorting a PIN diode connected across one of the coaxial capacitors. Thus, the coil was tuned when the PIN diodes were negatively biased. To improve the detuning of the volume coil during reception, the PIN diodes across each element were connected in series with inductors to form resonant tank circuits [21] as shown in Fig. 2. Tank circuits for ^{1}H and ^{31}P elements were tuned to produce high resistive impedances at 170 and 69 MHz, respectively. All the PIN diodes were connected in parallel through RF chokes and, therefore, could be activated simultaneously. A home-built PIN diode driver provided a current of about 100 mA per diode and a negative bias of −300 V. Additionally, instead of placing the PIN diodes near the back wall as in [19], they were mounted at the coil entrance where the capacitance of the TEM elements were adjusted to tune the tank circuits. Coaxial capacitors near the shielded back wall were utilized to tune the TEM volume coil using a procedure developed in our lab and described previously [22]. This procedure provides a more direct and efficient way to measure the distribution of RF current in all the TEM elements simultaneously as opposed to measuring the impedance of each individual resonance element individually [22].

We evaluated the effect of increasing the diameter of the volume coil (to accommodate the phased array) on the sensitivity of the volume coil. The sensitivity of the coils was evaluated by measuring the RF power required to produce a 90° square pulse in the transaxial slice in the center of a human head. The coil produced RF magnetic field of 1 kHz (23.5 μT) in amplitude per 1 kW of power at ^{1}H frequency and 1.1 kHz (63.8 μT) per 1 kW at ^{31}P frequency. The sensitivity decreased by ∼1 dB as compared to a smaller $^{1}H/^{31}P$ double-tuned TEM volume coil (element i.d. −28 cm, shield −33.5 cm, length −20 cm).

The ^{31}P phased array consisted of four 9×10 cm surface coils circumscribing the head at approximately 45° to horizontal and vertical axes. The coils were built using 6.4 mm wide copper tape and placed on acrylic holder of 20 cm in diameter, Fig. 1B. To accommodate various head sizes the holder was split into two halves with the position of the top portion being adjustable in the vertical direction. Depending on a head size, the distance between the coils located on the separate formers (i.e., isolation between coils #1 and # 2, and coils #3 and #4, Fig. 1B) was about 1.5–3.5 cm greater than the distance between the adjacent coils located

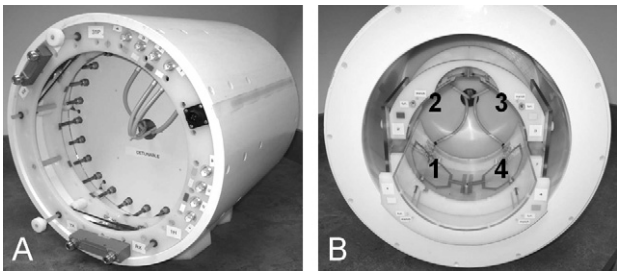

Fig. 1. (A) Back and (B) front views of $^{1}H/^{31}P$ actively detuneable TEM volume coil with the four-channel ^{31}P phased array located inside of the volume coil.

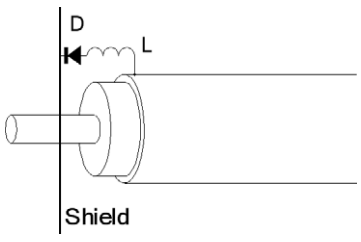

Fig. 2. Circuitry for the active detuning of the TEM volume coil. Inductor L forms a resonance tank circuit together with the coaxial capacitor of the TEM resonance element. When PIN diode D is shorted the tank circuit detunes the TEM element.

on the same former. When loaded with a human head, the intrinsic isolation between the coils on the top and bottom formers (coils #1 and #2, and coils #3 and #4) was −13 dB to −17 dB. The isolation between coils on the same former halves was initially −11 dB and improved by connecting a pair of small (~9 mm in diameter) loops in series with each surface coil [23] (Fig. 3). This produces a voltage of an opposite phase as compared to voltage induced due to mutual inductive coupling between the surface coils. After this inductive decoupling, the isolation between surface coils located on the same formers was better than −20 dB when loaded with either a head or a head-mimicking 2.0 L (50 mM NaCl) spherical phantom. This decoupling technique would be difficult to apply for the surface coils mounted on the different halves of the holder, which, however, was not required due to sufficient intrinsic isolation. For a phased array with a larger number of coils and smaller distances between them, preamplifier decoupling could be used to increase the inter-coil isolation [1,24]. Tri-axial baluns were used for each channel to prevent shield currents [5] (Fig. 3). To suppress cable interactions at both the ^{1}H and ^{31}P frequencies, the tri-axial baluns were constructed so as to provide high resistive impedance at both 69 and 170 MHz. The ratio of unloaded to loaded Q-factors (Q_U/Q_L) measured 290/75 on a human head for the ^{31}P surface coils located at the bottom part of the holder and 290/90 for the top surface coils. Introduction of the double-tuned triaxial baluns did not change the Q_U/Q_L ratio measured for a single surface coil on a human head and head-mimicking 2.0 L phantom (50 mM NaCl). All the surface coils were actively detuned using the PIN diode resonance tank circuit described previously [20,21]. The isolation between the TEM and surface coils at the ^{31}P frequency was more than −35 dB when the phased array was actively detuned and more than −45 dB when the TEM was actively detuned. Since detuning the tank circuits in both the volume coil and in the surface coils produce high impedance only at a single frequency (69 MHz in the surface coils or 170 MHz in the TEM) we also tested the isolation between the phased array and the volume coil at 170 MHz. With the array detuned, the isolation was greater than −30 dB and greater than −40 dB with the TEM detuned. With the phased array detuned, the isolation between ^{31}P and ^{1}H parts of the TEM measured about −25 dB at both frequencies. The power required to achieve a 90° square pulse with and without phased array inserted, was the same within the error of measurements (±1 dB). The absence of effect on the transmission efficiency also supports the effectiveness of the detuning network. We also evaluated the effectiveness of the phased array detuning by acquiring B_1 maps on a human head at the ^{1}H frequency with and without phased array inserted [25]. Both maps were practically the same and for that reason are not shown. The active detuning network for the phased array was constructed as shown in Fig. 3 and mounted on the shell of the volume coil (Fig. 1A). The network consisted of two sets of four BNC connectors (one set for each resonant frequency) located on the right side of the back of the TEM coil (Fig. 1A) and DC wiring to activate the PIN diodes. Thus, either a ^{31}P (69 MHz), or a ^{1}H (170 MHz) phased array, or even an array consisting of four double-tuned surface coils [26,27] for acquiring data at both frequencies could be used without repositioning the patient.

All images and spectroscopic data were acquired on a Varian INOVA 4 T whole-body system. ^{31}P spectroscopic images were acquired using a non-selective 37.5° excitation pulse and $13 \times 13 \times 13$ spherical encoding over a FOV of $24 \times 24 \times 24$ cm^3. The data was acquired using 6 averages and a TR of 0.5 s for an acquisition time of 48 min. The data was zero-filled to $16 \times 16 \times 16$, apodized with a Hanning filter and transformed in four dimensions (three spatial and one spectral) yielding an effective volume of ~9 cm^3.

RF safety was maintained by use of: (1) software calculations, (2) RF deposition measured at the amplifier and (3) maximum peak output limitations at the RF amplifier.

2.2. Double-tuned tri-axial baluns

A regular single-tuned tri-axial balun is typically constructed from a coaxial cable having two braids insulated from each other [5]. The outside shield is shorted with the inner shield at one quarter wavelength ($\lambda/4$) distance from the end of the cable. This produces high impedance between two braids at the resonance frequency and effectively suppresses the voltage from being induced across the cable due to coupling with the surface coil [5]. To construct a double-tuned tri-axial balun, high impedance between two braids is required at both frequencies of interest. The distance from the end of the cable to the position where braids were connected was chosen to be a few cm longer than the quarter wavelength at 170 MHz ($\lambda/4$ ~30 cm). The impedance measured at the end of the cable between the two cable shields at 170 MHz can be presented by its capacitive equivalent $1/j\omega C_1$, while at 69 MHz it has inductive equivalent of $j\omega L_1$ due the longer

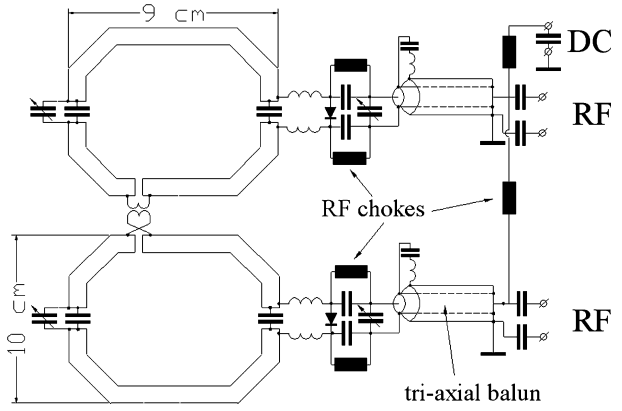

Fig. 3. Schematics of two surface coils including matching and PIN diode driving network. For simplicity only two surface coils located at the same portion of the coil holder are shown.

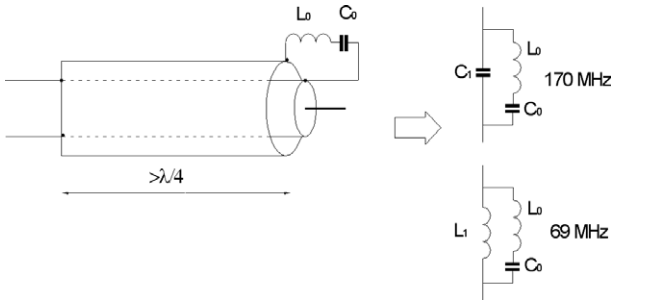

Fig. 4. Schematic of the double-tuned tri-axial balun with the series resonant circuit, formed by inductor L_0 and capacitor C_0, connected between two cable braids. Equivalent schematics of the entire circuit at both frequencies are shown on the right side.

Table 1
Parameters of the series resonance tank circuit

f_0 (MHz)	C_1 (pF)	L_1 (nH)	C_0 (pF)	L_0 (nH)
84.3	20.8	27.7	63.9	55.7

wavelength ($\lambda/4$ ~73 cm at 69 MHz). To produce high-impedance at both frequencies of interest, a series resonant circuit, formed by C_0 and L_0, was connected between the two shields as shown in Fig. 4. "Double tuning" of the balun is obtained when the impedance of this resonance circuit equals to $j/\omega C_1$ at 170 MHz and $-j\omega L_1$ at 69 MHz. Thus, L_0 and C_0 are given by

$$C_0 = \frac{\frac{1}{\omega_2^2} - \frac{1}{\omega_1^2}}{\frac{1}{\omega_1^2 C_1} + L_1}, \quad (1)$$

$$L_0 = \frac{1}{\omega_1^2}\left[\frac{1}{C_0} + \frac{1}{C_1}\right], \quad (2)$$

where $\omega_1 = 69$ MHz and $\omega_2 = 170$ MHz. Values of C_1 and L_1 were measured at 170 and 69 MHz, respectively, using a network analyzer in the impedance meter mode. L_1 and C_1 were measured individually for each of the four tri-axial baluns and then L_0 and C_0 were calculated using Eqs. (1) and (2). Table 1 presents an example of calculated values for one of the four tri-axial baluns where $\omega_0 = \frac{1}{\sqrt{C_0 L_0}}$ presents the resonance frequency of the series resonance circuit. Parameters calculated for the other baluns were within the range of 5–7% of the values shown in the table. Finally, the impedances of all the tank circuits were measured using a network analyzer and optimized by adjusting the inductance L_0. This method allowed us to effectively suppress cable interactions at both frequencies.

3. Results and discussion

Fig. 5 displays spectroscopic imaging data acquired using either the four-channel ^{31}P phased array or the TEM volume coil for reception from the same subject during the same session. In both cases the TEM volume coil was used for transmission. The spectroscopic data were reconstructed by summing the individually phased spectra weighted by its SNR [9]. Well resolved resonances from phosphocreatine, ATP, inorganic phosphate and phosphor mono- and di-esters are seen. These data were then compared to the data obtained by TEM volume coil used in transmit/receive (T/R) mode. For the locations 2, 4, 6 and 8 the major contribution to array data was from a single surface coil closest to the location. For locations 1, 3, 5 and 7, areas in the gaps between the coils, the signal is dominated by two coils. Finally, near the center of the brain, location 9, all four coils provided similar contributions. In comparison to the TEM volume coil, the SNR of the periphery of the brain near the surface coils improved threefold for the ^{31}P phased array, approximately twofold in the "gap areas", while similar sensitivity was achieved in the center of the brain. SNR in these "gap areas" can be further increased by adding more coil elements to the array and providing more complete coverage. Sensitivity near the center of the brain was near optimal

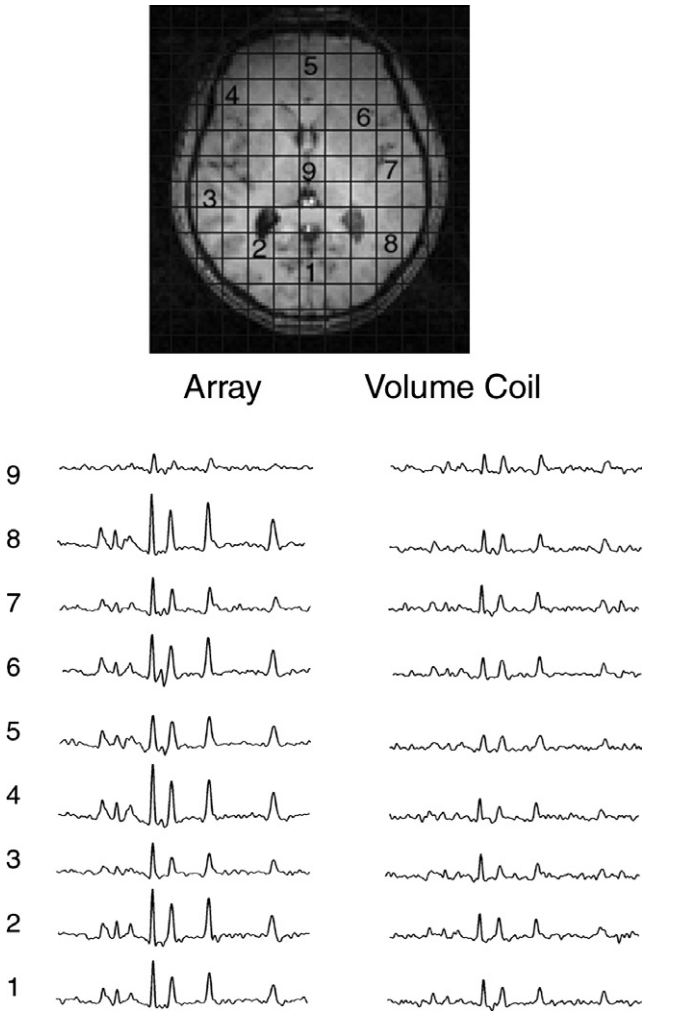

Fig. 5. Spectroscopic imaging data acquired using the four-channel ^{31}P phased array and the TEM volume coil for reception at 9 different locations in the periphery and the center of the human brain.

since it has been demonstrated previously that a phased array with full coverage of a head provided similar sensitivity as an optimized quadrature volume coil [10,28]. Since the ^{1}H portion of the volume coil can also be used for reception at the proton frequency, anatomical images from the entire brain can also be acquired in the same setting without the need for patient repositioning or changes in hardware configuration.

Our major goal was not to find an optimal SNR geometry for all types of applications but rather to overcome the technical difficulties associated with double-tuning the actively detuneable transmit coils and their use in conjunction with phased arrays. Depending upon the specific application the size, geometry and number of receiver coils to yield an "optimum result" whether it be homogeneity, localized SNR or acceleration for parallel imaging will vary, and has been extensively discussed in the literature [1,7–18] and remains an active area of research. In our case the number of elements in the array was limited by the number of receivers on our system ($n = 4$). However, the issues associated with surface coil decoupling in the case of different array geometries can be overcome using methods we applied in this work or other recipes previously described [1,29,30]. The inductive decoupling method we utilized in this work is similar in physical principle to coil overlapping [1] but can be applied for coils located at a distance and allows more accurate adjustment of the coil isolation by changing the distance between the decoupling loops. The loops were mounted at the opposite side of the acrylic holder away from a load (a human head). Moving the loops away from the load allowed us to preserve loaded Q-factors, Q_L by keeping sample losses unchanged. Loaded Q-factors, measured for an individual surface coil and a pair of coils with decoupling circuit installed, using the head-mimicking phantom were the same. Using this method previously to construct arrays consisted of surface coils of different size and geometry we were able to achieve very good (better than −20 dB) decoupling between adjacent nonoverlapping coils at various distances between the surface coils (as close as 1 cm) and various sizes of the surface coils (from about 7 to 14 cm). Varying the distance and the surface coil's size, however, requires adjustment of the size of the decoupling loops as well as coupling between them by adjusting the distance between the loops.

Due to limited in vivo sensitivity at ^{31}P frequency the accuracy of the measurements of the sensitivity of the phased array and the volume coil is limited. To access the sensitivity of the ^{31}P phased array we also utilized a ^{1}H phased array constructed identically. The ^{1}H portion of the TEM coil, which has the same geometry as the ^{31}P part of the TEM, was used as a reference. However, the field profiles of the surface and the volume coil change with increasing frequency due to interaction of the RF field with the tissue. For example, it has been reported that the asymmetry of the B_1 field profile of a 12 cm surface coil changes from 15% to 33% going from 1.5 T to 4 T [31]. The homogeneity of a head size volume coil also changes from ±5% to ±15% in going from 1.5 T to 4 T [6,20,22,32]. This alteration of the RF magnetic filed profile may complicate the use of ^{1}H data for quantitative assessment of sensitivities at the ^{31} P frequency, however, it still can be utilized for qualitative evaluation and optimization of the ^{31}P array geometry. As an example Fig. 6 demonstrates a map of a ratio of the SNR of the 4-channel ^{1}H phased array to the SNR obtained by the ^{1}H part of the double-tuned TEM volume coil. In spite of substantial differences in the frequency the values obtained were similar to measured at ^{31}P frequency for locations 1–8 shown in Fig. 5. The ratio between SNR values measured near the coils and in the "gaps" was about 20% larger for the ^{1}H array. This difference is within the expected error taking into account the difference in frequency and the larger voxel size for ^{31}P spectroscopic images.

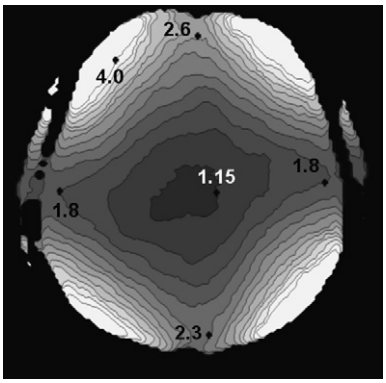

Fig. 6. Map of a ratio of the SNR of the 4-channel ^{1}H phased array to the SNR obtained by the ^{1}H part of the double-tuned TEM volume coil. ^{1}H phased array had the same size and geometry as the ^{31}P array described in the text.

In conclusion, an actively detuneable ^{31}P/^{1}H double-tuned TEM volume transmit/four-channel ^{31}P array receive RF system was developed for 4 T MRSI of the human brain. It can be used either in volume-transmit/array-receive mode or in TEM transmit/receive mode with the array detuned. Double-tuned tri-axial baluns constructed to provide high impedances between two insulated cable braids at both frequencies of interest allowed us effectively suppress shield currents and cable interaction at both 170 and 69 MHz.

Acknowledgment

This work was supported by NIH M01-RR12248, R01-EB00473, R21-EB005438.

References

[1] P.B. Roemer, W.A. Edelstein, C.E. Hayes, S.P. Souza, O.M. Mueller, The NMR phased array, Magn. Reson. Med. 16 (1990) 192–225.
[2] C.J. Hardy, P.A. Bottomley, K.W. Rohling, P.B. Roemer, An NMR phased array for human cardiac ^{31}P spectroscopy, Magn. Reson. Med. 28 (1992) 54–64.
[3] R.F. Lee, R. Giaquinto, C. Constantinides, S. Souza, R.G. Weiss, P.A. Bottomley, A broadband phased-array system for direct

phosphorus and sodium metabolic MRI on a clinical scanner, Magn. Reson. Med. 43 (2000) 269–277.
[4] D. Seeber, J. Jevtic, A. Menon, V. Pikelja, W. Johnson, Cable routing in MRI phased array coils, in: Proceedings of the 11th Annual Meeting of the ISMRM, Toronto, Canada, 2003, p. 426.
[5] C.-N. Chen, D.I. Hoult, Biomedical Magnetic Resonance Technology, Adam Hilger, Bristol and New York, 1989.
[6] J.T. Vaughan, H.P. Hetherington, J.O. Otu, J.W. Pan, G.M. Pohost, High frequency volume coils for clinical NMR imaging and spectroscopy, Magn. Reson. Med. 32 (1994) 206–218.
[7] L.L. Wald, S.E. Moyher, M.R. Day, S.J. Nelson, D.B. Vigneron, Proton spectroscopic imaging of the human brain using phased array detectors, Magn. Reson. Med. 34 (1995) 440–445.
[8] P.A. Bottomley, C.H. Lugo Olivieri, R. Giaquinto, What is the optimum phased array coil design for cardiac and torso magnetic resonance? Magn. Reson. Med. 37 (1997) 591–599.
[9] S.M. Wright, L.L. Wald, Theory and application of array coils in MR spectroscopy, NMR Biomed. 10 (1997) 394–410.
[10] J.R. Porter, S.M. Wright, A. Reykowski, A 16-element phased-array head coil, Magn. Reson. Med. 40 (1998) 272–279.
[11] B. deB Frederick, L.L. Wald, L.C. MaasIII, P.F. Renshaw, A phased array echoplanar imaging system for fMRI, Magn. Reson. Imag. 17 (1999) 121–129.
[12] M. Nittka, A. Haase, Investigation of complex phased array coil designs for cardiac imaging, MAGMA 10 (2000) 122–130.
[13] R.F. Lee, C.R. Westgate, R.G. Weiss, D.C. Newman, P.A. Bottomley, Planar strip array (PSA) for MRI, Magn. Reson. Med. 45 (2001) 673–683.
[14] M. Weiger, K.P. Pruessmann, C. Leussler, P. Roschmann, P. Boesiger, Specific coil design for SENSE: a six-element cardiac array, Magn. Reson. Med. 45 (2001) 495–504.
[15] J.A. Bankson, S.M. Wright, Simulation-based investigation of partially parallel imaging with a linear array at high accelerations, Magn. Reson. Med. 47 (2002) 777–786.
[16] R. Brown, A. Mareyam, E. Reid, Y. Wang, Novel RF coil geometry for lower extremity imaging, Magn. Reson. Med. 51 (2004) 635–639.
[17] A.O. Rodriguez, L. Medina, Improved SNR of phased-array PERES coils via simulation study, Phys. Med. Biol. 50 (2005) N215–N225.
[18] C.J. Hardy, H.E. Cline, R.O. Giaquinto, T. Niendorf, A.K. Grant, D.K. Sodickson, 32-element receiver-coil array for cardiac imaging, MRM 55 (2006) 1142–1149.
[19] J.T. Vaughan, G. Adriany, M. Garwood, T. Yacoub, T. Duong, L. DelaBarre, P. Andersen, K. Ugurbil, Detunable Transverse Electromagnetic (TEM) volume coil for high field NMR, Magn. Reson. Med. 47 (2002) 990–1000.
[20] N.I. Avdievich, H.P. Hetherington, A 4 T Actively detunable transmit/receive ^{1}H transverse electromagnetic (TEM) and 4-channel receive-only phased array for ^{1}H human brain studies, Magn. Reson. Med. 52 (2004) 1459–1464.
[21] W.A. Edelstein, C.J. Hardy, O.M. Mueller, Electronic decoupling of surface-coil receivers for NMR imaging and spectroscopy, J. Magn. Reson. 67 (1986) 156–161.
[22] N.I. Avdievich, V.N. Krymov, H.P. Hetherington, Modified perturbation method for transverse electromagnetic (TEM) coil tuning and evaluation, Magn. Reson. Med. 50 (2003) 13–18.
[23] P. Brown, Yale University, private communication.
[24] J.A. de Zwart, P.J. Ledden, P. Kellman, P. van Gelderen, J.H. Duyn, Design of a SENSE-optimized high-sensitivity MRI receive coil for brain imaging, Magn. Reson. Med. 47 (2002) 1218–1227.
[25] J.W. Pan, D.B. Twieg, H.P. Hetherington, Quantitative spectroscopic imaging of the human brain, Magn. Reson. Med. 40 (1998) 363–369.
[26] M.D. Schnall, V.H. Subramanian, J.S. Leigh, B. Chance, A new double-tuned probe for concurrent ^{1}H and ^{31}P NMR, J. Magn. Reson. 65 (1985) 122–129.
[27] G. Muda, van H. Laarhoven, D. Klomp, J. Pikkemaat, J. van Asten, Y. Kamm, A. Heerschap, Double tuned coil for interleaved ^{31}P/^{19}F MRS of mouse tumors at 7 Tesla, in: Proceedings of the 9th Annual Meeting of the ISMRM, Glasgow, Scotland, 2001, p. 1106.
[28] T. Schäffter, P. Börnert, C. Leussler, I.C. Carlsen, D. Leibfritz, Fast ^{1}H spectroscopic imaging using a multi-element head-coil array, Magn. Reson. Med. 40 (1998) 185–193.
[29] R.G. Pinkerton, E.A. Barberi, R.S. Menon, Transceive surface coil array for magnetic resonance imaging of the human brain at 4 T, Magn. Reson. Med. 54 (2005) 499–503.
[30] R.F. Lee, R.O. Giaquinto, C.J. Hardy, Coupling and decoupling theory and its application to the MRI phased array, Magn. Reson. Med. 48 (2002) 203–213.
[31] J.R. Keltner, J.W. Carlson, M.S. Roos, S.T.S. Wong, T.L. Wong, T.F. Budinger, Electromagnetic fields of surface coil in vivo NMR at high frequencies, Magn. Reson. Med. 22 (1991) 467–480.
[32] J. Jin, J. Chen, On the SAR and field inhomogeneity of birdcage coils loaded with the human head, Magn. Reson. Med. 38 (1997) 953–963.